



ELSEVIER

Contents lists available at ScienceDirect

Inorganica Chimica Acta

journal homepage: www.elsevier.com/locate/ica

Research paper

Photodynamic inactivation of *Enterococcus faecalis* by conjugates of zinc(II) phthalocyanines with thymol and carvacrol loaded into lipid vesiclesLukasz Sobotta^{a,*}, Sebastian Lijewski^b, Jolanta Długaszewska^c, Joanna Nowicka^a,
Jadwiga Mielcarek^a, Tomasz Goslinski^b^a Department of Inorganic and Analytical Chemistry, Poznan University of Medical Sciences, Grunwaldzka 6, 60-780 Poznan, Poland^b Department of Chemical Technology of Drugs, Poznan University of Medical Sciences, Grunwaldzka 6, 60-780 Poznan, Poland^c Department of Genetics and Pharmaceutical Microbiology, Poznan University of Medical Sciences, Swiecickiego 4, 60-781 Poznan, Poland

ARTICLE INFO

Keywords:

Phthalocyanines

Singlet oxygen

PACT

Terpenes

Enterococcus faecalis

ABSTRACT

Terpene-macrocycle conjugates, consisting of thymol or carvacrol and phthalocyanine were synthesized, characterized, and subjected to detailed optical and biological studies. The macrocyclization reactions of terpene-substituted *o*-phthalonitrile derivatives were performed in a microwave reactor to give thymol- and carvacrol-phthalocyanine conjugates, which were carefully purified by column chromatography and subsequently analyzed using HPLC and characterized using UV–Vis, NMR and MS. Both isolated phthalocyanine derivatives represent isomers of C_{2v} symmetry, which was confirmed by NMR study. The absorption UV–Vis spectra of studied thymol- and carvacrol-phthalocyanine conjugates with the Soret and the Q band possesses the same profile. Both molecules reveal emission in the red region of the spectrum with fluorescence quantum yields about two-fold lower in DMF and significantly lower in DMSO than that observed for zinc(II) phthalocyanine. The analyzed phthalocyanine derivatives generate singlet oxygen upon excitation with light at ca. three-fold lower level than that noticed for zinc(II) phthalocyanine. In comparison to zinc(II) phthalocyanine, both molecules also reveal two-fold lower photostability in DMF and similar stability in DMSO. Thymol- and carvacrol-phthalocyanine conjugates, zinc(II) phthalocyanine, thymol, and carvacrol were loaded into modified liposomes and subjected to biological activity study. Thymol-phthalocyanine conjugate at both 100 and 10 μM revealed high, ca. 5 log photoinactivation potential on the growth of *Enterococcus faecalis*, similarly to reference zinc(II) phthalocyanine. For carvacrol-phthalocyanine conjugate, an increase of photoinactivation activity was observed at only 100 μM in comparison to zinc(II) phthalocyanine, whereas a decrease at the concentration of 10 μM was noticed. It is crucial that both studied phthalocyanines cross the border of 3 log photoinactivation potential, which indicates their bactericidal potential. In the Microtox® bioassay both conjugates revealed significantly decreased dark toxicity in comparison to thymol and carvacrol only. Interestingly, the carvacrol-phthalocyanine conjugate was found to be more toxic in comparison to thymol-phthalocyanine conjugate and zinc(II) phthalocyanine.

1. Introduction

Phthalocyanines (Pcs) are tetrapyrrolic macrocycles possessing a vast spectrum of applications [1,2]. Pcs exhibit the ability to generate reactive oxygen species, including extremely reactive singlet oxygen, upon irradiation with visible light. They have been considered as promising photosensitizers in photodynamic therapy (PDT) and photodynamic antimicrobial chemotherapy (PACT) [3–5]. In PDT, phthalocyanines underwent clinical trials for the treatment of tumors and age-related macular degeneration, for example, aluminum(III) sulfonated phthalocyanine applied as Photosens®. PACT has also been considered

as a new strategy to destroy antibiotic-resistant microorganisms as the Golden Age of antibiotics seems to be coming dusk [6,7]. Many phthalocyanines have revealed photodynamic antimicrobial activity in a plethora of preclinical trials. Pcs have been considered as very efficient and stable photosensitizers for PACT. The limitations which should be overcome to broaden their more extensive usage in therapy are their hydrophobicity and tendency to form aggregates in solution [8]. Many studies revealed that the connection of phthalocyanines with novel drug delivery systems or nanostructures, as well as proper peripheral functionalization or conjugation with other molecules could improve the effectiveness of PACT. Some phthalocyanines, including

* Corresponding author.

E-mail address: lsobotta@ump.edu.pl (L. Sobotta).<https://doi.org/10.1016/j.ica.2019.02.031>

Received 8 January 2019; Received in revised form 21 February 2019; Accepted 22 February 2019

Available online 23 February 2019

0020-1693/ © 2019 Published by Elsevier B.V.

amphiphilic sulphonated zinc(II), cationic methylpyridinium aluminum (III), cationic indium(III) derivatives revealed differentiated antibacterial activity against *Staphylococcus aureus*, *Escherichia coli* and *Candida albicans* [9,10]. Especially, PACT with cationic phthalocyanines has been found effective against various bacteria planktonic and biofilm cultures, including *E. coli* [11] and *S. aureus* [12]. Silicon(IV) phthalocyanines have revealed photoinactivation potential against *E. coli* cultures [13] and *C. albicans* [14,15]. Also, various zinc(II) phthalocyanines conjugated with an oligolysine chains showed interesting PACT potential against different strains of *S. aureus*, *E. coli* and *P. aeruginosa* [16,17]. PACT potential can also be significantly strengthened by proper pharmaceutical formulation, using emulsions and liposomes. For example, photodynamic inactivation of *Cryptococcus neoformans* melanized cells up to 6-log in survival was achieved with chloroaluminum phthalocyanine emulsion in the *in vitro* study [18]. In our latest studies, we have also demonstrated *in vitro* photodynamic activity potential of zinc(II) phthalocyanine substituted with 2-propoxy substituents and pyrrolyl-substituted zinc(II) porphyrazine and chlorins incorporated into modified liposome vesicles against *Enterococcus faecalis* [19–23].

The genus *Enterococcus* comprises a ubiquitous group of Gram-positive bacteria that inhabit the gastrointestinal tract, oral cavity, and vagina of mammal's [24]. Moreover, these microorganisms are common in the environment, as well as in dairy and meat products [25,26]. The majority Enterococcal infections are caused by *Enterococcus faecalis* (80–90%) followed *Enterococcus faecium* (10%). *Enterococci* cause a range of infections in the community setting (including pelvic, neonatal and urinary tract infections), infective endocarditis, hospital-acquired infections, as well as dental infections. In dentistry, *Enterococcus* species, in particular, *Enterococcus faecalis*, are associated with chronic periodontitis and failed root canal treatments [27,28]. It is believed that *enterococci* can survive harsh conditions such as a wide pH range and nutrient-limited conditions and persist within the root canal system after treatment. Moreover, *enterococci* demonstrate intrinsic resistance to common antibiotics, including all generations of cephalosporins, clindamycin, trimethoprim-sulfamethoxazole, and aminoglycosides at low concentrations. Also, they can acquire resistance to glycopeptides, quinupristin-dalfopristin, daptomycin, linezolid, as well as high-level aminoglycosides and ampicillin resistance [29]. As traditional antibiotic therapy is not always effective, novel approaches, including antimicrobial photodynamic therapy are worthy of further investigations.

In our current study, we decided to obtain terpene-phthalocyanine conjugates. The rationale for such approach is related to known pharmacological and physicochemical properties of terpenes. Terpenes constitute a large family of organic compounds produced mainly by plants. In nature, they serve as plant protection from microorganisms, parasites, and herbivores. Terpenes are also biologically crucial since e.g. carotenoids or vitamin A belong to terpenes. Herbs containing terpenes have been known and used in traditional medicine since ancient times. e.g., chamomile is used in many soothing creams, ointments, and cosmetics. Among many properties like anti-inflammatory or antimicrobial activity, terpenes (e.g. azulene) have been proved to possess photosensitizing potential [30,31]. Thymol is a naturally occurring phenol monoterpene derivative constituting one of the major constituents of essential oils of medicinal plant thyme (*Thymus vulgaris*) [32]. Carvacrol is a phenolic monoterpene found in essential oils of oregano (*Origanum vulgare*), thyme (*Thymus vulgaris*), wild bergamot (*Citrus aurantium bergamia*) and other plants [33]. Thymol and carvacrol have well known antimicrobial and antifungal activity. Also, they have been considered as alternative antimicrobial agents against antibiotic-resistant pathogenic bacteria [34], and as a possible food preservative or components of polymer films for antimicrobial food packaging [35,36]. The interest is related in developing technology to produce nanoscale systems for delivering lipophilic components in aqueous foods, e.g. in this way nanodispersions containing thymol at

concentrations well above its solubility limit using the emulsion- evaporation technique were developed [37]. Also, the antimicrobial activity of nanodispersed thymol in tryptic soy broth was analyzed in comparison to free thymol. The study demonstrated that transparent nanodispersions of thymol have promising antimicrobial activity against a broad spectrum of foodborne pathogens [38]. In a similar study, nanodispersed eugenol has revealed improved antimicrobial activity against *E. coli* O157:H7 and *Listeria monocytogenes* in bovine milk [39]. Mutual prodrugs of ibuprofen with menthol, thymol, and eugenol have been selected with the aim of getting a synergistic effect. These prodrugs have showed increased anti-inflammatory activity that has been attributed to the synergistic effect as ibuprofen conjugates to natural analgesics [40]. Moreover, some sulfamethoxazole conjugates with monocyclic terpenes, like thymol and eugenol have revealed potent antibacterial activity and have been more active than individual terpenes, against multidrug-resistant (MDR) gruesome pathogenic bacteria [41]. In a similar study, the thymol-sulfadiazine conjugate has been found to be effective antibacterial against gruesome MDR bacteria [42]. There are also known some photosensitizer-antibiotic conjugates with antibacterial activity, including Rose bengal-penicillanic acid, Rose bengal-linker-penicillanic acid and Rose bengal-linker-kanamycin against *Staphylococcus aureus* and *Escherichia coli*. The highest eradication of *S. aureus* and *E. coli* was observed for Rose bengal-linker-kanamycin [43]. Hence, conjugation of phthalocyanine macrocycle with terpene moiety could result with a compound of improved physical-chemical properties and a high potency in photodynamic therapy, especially against microorganisms (PACT) we decided to obtain and characterize novel terpene-phthalocyanine analogs in this study.

2. Experimental

2.1. General procedures

All reactions were conducted in oven-dried glassware under an argon atmosphere using the Radleys Heat-On heating system. Microwave-assisted synthesis of macrocycles was conducted in an Anton Paar Monowave 400 reactor. All solvents were rotary evaporated at or below 50 °C under reduced pressure. Flash column chromatography was carried out on Merck silica gel, particle size 40–63 µm. Reversed-phase chromatography was carried out on Fluka C18 silica gel 90 (particle size 40–63). Thin layer chromatography (TLC) was performed on silica gel Merck Kieselgel 60 F₂₅₄ plates and visualized with UV illumination (λ_{\max} 254 or 365 nm). UV-Vis spectra were recorded on a Hitachi UV/VIS U-1900 and Shimadzu UV-160A spectrophotometers. ¹H NMR, ¹³C NMR spectra were prepared using a Bruker Avance II spectrometer operating at 400.13 MHz for ¹H and 100.61 MHz for ¹³C and Bruker Avance III spectrometer operating at 500.25 MHz for ¹H and 125.79 MHz for ¹³C at the Institute of Bioorganic Chemistry Polish Academy of Sciences in Poznan. Chemical shifts (δ) are quoted in parts per million (ppm) and referred to a residual solvent peak. Coupling constants (*J*) are quoted in Hertz (Hz). The abbreviations s, d, t, m refer to a singlet, doublet, triplet and multiplet, respectively. Mass spectra (ESI) were recorded at Bruker Impact HD ESI-Q-TOF mass spectrometer at the Wielkopolska Centre for Advanced Technologies in Poznan.

2.2. Synthetic procedures

All reagents were purchased from commercial suppliers and used without additional purification. 1-Azulenecarbaldehyde was synthesized adopting literature method [44].

2.2.1. (2Z)-2-Amino-3-{[azulen-1-ylmethylidene]amino}but-2-enedinitrile (2)

1-Azulenecarbaldehyde (849 mg, 5.4 mmol) and diaminomaleonitrile 1 (486 mg, 4.5 mmol) were dissolved in anhydrous methanol

(20 mL). Careful addition of trifluoroacetic acid (0.4 mL) resulted with precipitation of brown solid. Next, the obtained solid was filtered, washed with methanol and chromatographed (CH₂Cl₂:methanol, 50:1, v/v) to give **2** as a dark brown solid (0.969 g, 90% yield); m.p. 205 °C. R_f (CH₂Cl₂:methanol, 50:1, v/v) 0.33. UV–Vis (CH₂Cl₂) λ_{max} nm (log ε) = 289 (3.51), 337 (3.64), 439 (4.02), 613 (2.85). ¹H NMR (400.15 MHz, DMSO-*d*₆) δ: 9.30 (d, ³J = 10.0 Hz, 1H), 8.77 (s, 1H), 8.54 (d, ³J = 9.5 Hz, 1H), 8.50 (d, ³J = 4.0 Hz, 1H), 7.91 (t, ³J = 10.0 Hz, 1H), 7.62–7.43 (m, 5H). ¹³C NMR (100.63 MHz, DMSO-*d*₆) δ: 150.3, 145.3, 140.1, 139.3, 138.4, 138.4, 136.8, 127.7, 127.3, 124.6, 123.9, 119.9, 115.2, 114.1, 105.4. MS (ES pos): *m/z* 247 [M + H]⁺, 269 [M + Na]⁺, 285 [M + K]⁺. MS (ES neg): *m/z* 245 [M + H]⁻.

2.2.2. (2*Z*)-2-[(Azulen-1-ylmethyl)(methyl)amino]-3-(dimethylamino)but-2-enedinitrile (**3**)

Compound **2** (738 mg, 3 mmol) was suspended in methanol (50 mL) and sodium borohydride (456 mg, 12 mmol) was added in small portions until substrate dissolved completely. Mixture was poured on water with ice mixture (1:1). Resulting precipitate was washed with water, dried and chromatographed (CH₂Cl₂:methanol, 50:1, v/v) to give dark brown solid (677 mg, 91% yield); R_f (CH₂Cl₂:methanol, 50:1, v/v) 0.38; UV–Vis (CH₂Cl₂) λ_{max} nm 289, 439. Resulting amine was highly unstable and was immediately applied in the next step. Sodium hydride (60% dispersion in mineral oil, 87 mg, 3.62 mmol) was suspended in anhydrous dimethylformamide (7.5 mL) at -18 °C. After 30 min the amine substrate (409 mg, 1.65 mmol) dissolved in dimethylformamide (2.5 mL) was added dropwise during 30 min. Next, dimethyl sulfate (349 μL, 3.62 mmol) dissolved in dimethylformamide (0.5 mL) was added dropwise. After 2 h mixture was poured on water with ice, and the resulting precipitate was washed with water, dried and chromatographed (CH₂Cl₂:methanol, 50:1, v/v) to give **3** as a dark brown solid (174 mg, 36% yield); m.p. 205 °C. R_f (*n*-hexane:ethyl acetate, 7:2, v/v) 0.3. UV–Vis (CH₂Cl₂) λ_{max} nm 232, 288, 452, MS (ES) *m/z* 275 [M - CH₃]⁺, 313 [M + Na]⁺. Unfortunately, compound **3** was found to be very unstable during physicochemical characterization and subsequent macrocyclization reaction (magnesium *n*-butanolate in *n*-butanol).

2.2.3. 3-[5-Methyl-2-(propan-2-yl)phenoxy]benzene-1,2-dicarbonitrile (**5**) (modification of the literature approach [45])

Anhydrous K₂CO₃ (4.1 g, 30 mmol), was added to a well stirred slurry of thymol (1.35 g, 9 mmol) and 3-nitroptalonitrile **4** (0.43 g, 3 mmol) in DMF (8 mL) and heated at 70 °C for 24 h. After cooling to room temperature the reaction mixture was poured into water and ice mixture (1:1, 300 mL). The resulting precipitate was filtrated, washed with distilled water (3 × 100 mL) and chromatographed (CH₂Cl₂:methanol, 50:1, v/v) to give **5** as light yellow solid (0.69 g, 83% yield); m.p. 95 °C. R_f (CH₂Cl₂) 0.56. UV–Vis (CH₂Cl₂) λ_{max} nm (log ε): 228 (3.79), 319 (4.29). ¹H NMR (400.13 MHz, DMSO-*d*₆) δ: 7.80 (s, 1H), 7.79 (d, ³J = 1.5 Hz, 1H), 7.34 (d, ³J = 8.0 Hz, 1H), 7.14 (m, 1H), 7.11 (m, 1H), 6.93 (s, 1H), 2.98 (m, 1H), 2.27 (s, 3H), 1.14 (d, ³J = 7.0 Hz, 6H). ¹³C NMR (100.61 MHz, DMSO-*d*₆) δ: 160.3, 150.5, 137.5, 136.5, 136.1, 127.7, 127.5, 127.3, 120.9, 120.7, 115.9, 115.6, 113.4, 104.2, 26.7, 22.8, 20.3. MS (ESI): *m/z* 277 [M + H]⁺, 299 [M + Na]⁺. HRMS (ESI): *m/z* calcd. for (C₁₈H₁₆N₂O): 277.1341 [M + H]⁺; found: 277.1328 [M + H]⁺.

2.2.4. 3-[2-Methyl-5-(propan-2-yl)phenoxy]benzene-1,2-dicarbonitrile (**6**)

Anhydrous K₂CO₃ (4.1 g, 30 mmol), was added to a well stirred slurry of carvacrol (1.35 g, 9 mmol) and 3-nitroptalonitrile **4** (0.43 g, 3 mmol) in DMF (8 mL) and heated at 70 °C for 24 h. After cooling to room temperature the reaction contents were poured into water and ice mixture (1:1, 300 mL). The resulting precipitate was filtrated, washed with distilled water (3 × 100 mL) and chromatographed (CH₂Cl₂:methanol, 50:1, v/v) to give **6** as a light yellow solid (0.56 g, 68% yield); m.p. 63 °C. R_f (*n*-hexane:ethyl acetate, 7:2, v/v) 0.48.

UV–Vis (CH₂Cl₂) λ_{max} nm (log ε) = 228 (3.69), 319 (4.15). ¹H NMR (400.13 MHz, DMSO-*d*₆) δ: 7.80 (s, 1H), 7.79 (s, 1H), 7.32 (d, ³J = 8.0 Hz, 1H), 7.15 (d, ³J = 8.0 Hz, 1H), 7.06 (s, 1H), 7.02 (m, 1H), 2.88 (m, 1H), 2.10 (s, 3H), 1.18 (d, ³J = 7.0 Hz, 6H). ¹³C NMR (100.61 MHz, DMSO-*d*₆) δ: 160.1, 151.3, 149.0, 136.1, 131.9, 127.5, 126.7, 124.4, 120.1, 118.7, 115.9, 115.6, 113.3, 103.8, 32.9, 23.7, 15.0. MS (ESI): *m/z* 277 [M + H]⁺, 299 [M + Na]⁺. HRMS (ESI): *m/z* calc. for (C₁₈H₁₆N₂O): 277.1341 [M + H]⁺; found: 277.1332 [M + H]⁺.

2.2.5. {1,8,18,25-Tetrakis[5-methyl-2-(propan-2-yl)phenoxy]phthalocyanine}zinc(II) (**7**)

n-Pentanol (1 mL), zinc acetate (0.18 g, 1 mmol) and **5** (0.55 g, 2 mmol) were placed in a G10 vial. The vial was filled with argon and sealed. Reaction was conducted in a microwave reactor at 200 °C for 15 min. Next, reaction mixture was filtered, the solid was washed with toluene and the combined filtrates were evaporated. The dark green residue was chromatographed using silica gel (CH₂Cl₂:methanol, 50:1, v/v) and C-18 reversed-phase gel (methanol, then CH₂Cl₂) to give **7** as a dark green solid (0.11 g, 19% yield); m.p. 235 °C. R_f (CH₂Cl₂:methanol, 50:1, v/v) 0.23. UV–Vis (CH₂Cl₂) λ_{max} nm (log ε) = 227 (4.41), 327 (4.39), 633 (4.29), 703 (5.04), 747 (4.24). ¹H NMR (500.25 MHz, pyridine-*d*₅) δ: 9.62 (d, ³J = 7.5 Hz), 9.55 (m), 9.35 (m), 8.2 (t, ³J = 7.5 Hz), 8.09 (m), 7.98 (t, ³J = 7.5 Hz), 7.66 (m), 7.42 (s), 7.36 (s), 7.35 (s), 7.25 (s), 4.07 (m, 1H), 3.69 (s, 1H), 2.24 (m, 6H), 1.64 (m, 6H), 1.14 (m, 6H). ¹³C NMR (125.79 MHz, pyridine-*d*₅) δ: 158.2, 158.1, 156.1, 156.0, 156.0, 155.3, 155.2, 155.2, 155.1, 155.0, 154.9, 154.9, 154.8, 154.8, 154.7, 154.5, 154.3, 142.7, 142.6, 142.6, 142.5, 142.4, 142.3, 139.1, 138.0, 138.0, 137.9, 137.9, 137.8, 131.8, 131.6, 131.4, 128.3, 128.2, 128.1, 127.9, 127.5, 127.4, 127.2, 127.2, 126.9, 126.8, 126.3, 126.2, 121.7, 121.6, 121.6, 118.7, 118.6, 118.5, 118.4, 117.5, 117.3, 117.2, 117.1, 28.7, 27.6, 24.0, 23.8, 21.4, 21.3. MS (ESI): *m/z* 1169 [M + H]⁺. HRMS (ESI): *m/z* calcd. for (C₇₂H₆₄N₈O₄Zn): 1169.4420 [M + H]⁺; found: 1169.4404 [M + H]⁺. HPLC (see [Supporting Information](#)).

2.2.6. {1,8,18,25-Tetrakis[2-methyl-5-(propan-2-yl)phenoxy]phthalocyanine}zinc(II) (**8**)

n-Pentanol (1 mL), zinc acetate (0.18 g, 1 mmol) and **6** (0.55 g, 2 mmol) were placed in a G10 vial. The vial was filled with argon and sealed. Reaction was conducted in a microwave reactor at 200 °C for 15 min. Next, reaction mixture was filtered, the solid was washed with toluene and filtrates were evaporated. Dark green residue was chromatographed using silica gel (CH₂Cl₂:methanol, 50:1, v/v) and C-18 reversed-phase gel (methanol, then CH₂Cl₂) to give **8** as a dark green solid (0.08 g, 13% yield); m.p. 227 °C. R_f (CH₂Cl₂:methanol, 50:1, v/v) 0.34. UV–Vis (CH₂Cl₂) λ_{max} nm (log ε) = 228 (4.60), 327 (4.51), 632 (4.40), 702 (4.99), 745 (4.37). ¹H NMR (500.25 MHz, pyridine-*d*₅) δ: 9.63 (m), 9.58 – 9.50 (m), 9.37 (t, ³J = 7.5 Hz), 9.27 (t, ³J = 7.0 Hz), 8.20 (m), 8.10 (m), 8.03 (m), 7.92 (t, ³J = 7.6 Hz), 7.73 (d, ³J = 7.8 Hz), 7.68 – 7.60 (m), 7.56 (s), 7.50 (m), 7.43 – 7.37 (m), 7.33 (s), 7.19 (m), 7.17 – 7.09 (m), 2.91 – 2.82 (m), 2.82 – 2.74 (m), 2.35 – 2.24 (m), 1.27 – 1.18 (m), 1.09 (m). ¹³C NMR (125.79 MHz, pyridine-*d*₅) δ: 158.1, 156.1, 156.0, 156.0, 155.3, 155.2, 155.2, 155.1, 155.0, 154.9, 154.9, 154.8, 154.8, 154.7, 154.5, 154.3, 142.7, 142.6, 142.6, 142.5, 142.4, 142.3, 139.1, 138.0, 138.0, 137.9, 137.9, 137.8, 131.8, 131.6, 131.4, 128.3, 128.2, 128.1, 127.9, 127.5, 127.4, 127.2, 127.2, 126.9, 126.8, 126.3, 126.2, 121.7, 121.6, 121.6, 118.7, 118.6, 118.5, 118.4, 117.5, 117.3, 117.2, 117.1, 28.7, 27.6, 24.0, 23.8, 21.4, 21.3. MS (ESI): *m/z* 1169 [M + H]⁺. HRMS (ESI): *m/z* calcd. for (C₇₂H₆₄N₈O₄Zn): 1169.4420 [M + H]⁺; found: 1169.4426 [M + H]⁺. HPLC (see [Supporting Information](#)).

2.3. Spectral properties

Absorption spectra were recorded with Hitachi UV/VIS U-1900 and Shimadzu UV-160A spectrophotometers in DMF and DMSO at ambient

temperature. Emission spectra were recorded with a Jasco 6200 spectrofluorometer in DMF and DMSO at ambient temperature. Fluorescence quantum yields were determined according to the methods described earlier. As a reference it was used unsubstituted zinc (II) phthalocyanine (**ZnPc**) with known fluorescence quantum yields equal 0.20 and 0.17 for DMF and DMSO respectively [46–49].

2.4. Singlet oxygen formation

Singlet oxygen generation quantum yields were evaluated in DMF and DMSO solutions at ambient temperature. Measurements were conducted according to the comparative method using a chemical quencher of singlet oxygen (DPBF) and a reference compound (**ZnPc**). The mixture of DPBF and a photosensitizer was irradiated with light adjusted to the maximum absorbance in the Q band of Pc spectrum. Spectrum changes were monitored with OceanOptics Flame Spectrometer and light source DT-MINI-2-GS. The quantum yields of singlet oxygen formation were calculated according to equation presented earlier [46,48–51].

2.5. Photostability determination

Photostability determination was performed in DMF and DMSO in aerobic condition at ambient temperature according to the method previously described. A xenon lamp (150 W, Optel) was used as a light source. Visible light was separated with cutting filter. Spectrum changes were monitored with OceanOptics Flame Spectrometer and light source DT-MINI-2-GS. The quantum yields of photodecomposition process were calculated according to the earlier presented equation [46,50,52,53].

2.6. Modified lipid vesicles preparation

Lipid vesicles were obtained by the method described by Dragicevic-Curic and co-workers [54]. POPC (1-palmitoyl-2-oleoyl-*sn*-glycero-3-phosphocholine) and DOTAP (N-[1-(2,3-dioleoyloxy)propyl]-N,N,N-trimethylammonium chloride, 25 mg/ml) purchased from Avanti Polar Lipids Inc. (Alabaster, AL, USA) were dissolved in chloroform (Aldrich) and mixed in a molar ratio of 8:2. In the next step 7, 8, thymol and carvacrol chloroform solutions at the concentration of 1 mg/ml were added in a proper amount to achieve the final concentration in the vesicle 100 and 10 μ M. Simultaneously, there were prepared “empty” liposomes. Then, the obtained mixture was evaporated under reduced pressure to give thin lipid film. Next, ethanol (3.3% w/v) was added, and vortexing for 5 min was performed. Further, the saline buffer was added, and vortexing for 5 min continued. The unification was performed by the extrusion of the mixture through the polycarbonate filter (200 nm). The size of obtained vesicles was measured with NanoSight LM10 (Malvern).

2.7. In vitro photodynamic antibacterial activity

Enterococcus faecalis strain was purchased from American Type Culture Collection (ATCC; *E. faecalis* ATCC 29212) and cultured aerobically in BHI broth at 36 ± 1 °C for 18–20 h. After this time microorganisms were harvested by centrifugation (3000G for 15 min) and resuspended in 10 mM phosphate buffered saline (PBS, pH = 7.0) and diluted in PBS to a final concentration of ca. 10^7 colony forming units (CFU)/mL.

2.8. Dark activity

Aliquots of a microbial suspension were placed in the microtitration plate and then solutions containing compounds incorporated in liposomal formulations were added and incubated for 20 min. Next bacterial suspension from each well, after dilution, was inoculated on

tryptic soy agar (TSA) plates. After an incubation period (20 h at 36 ± 1 °C), the number of colony was counted and the number of viable bacteria (colony forming units; CFUs) in 1 mL was calculated. A control study in darkness without studied compounds was performed simultaneously. The results were expressed as \log_{10} [CFU/ml]. The reduction of living bacteria in each sample was determined by the calculation log reduction factors (RF) as follows:

$RF = \text{Log } L(-)P(-) - \text{Log } L(-)P(+)$, where $L(-)P(-)$ – no irradiation, no Pc+ (negative control); $L(-)P(+)$ – no irradiation, Pc+ (dark control).

2.9. Light-dependent activity

Light activity evaluation was performed similarly to the dark one, with irradiation of the culture after an incubation time of 20 min. Bacteria were irradiated at room temperature with high power LED MultiChip Emitters (60 high-efficiency AlGaAs diode chips, Roithner LaserTechnik GmbH, Vienna, Austria) with maximum wavelength 690 ± 15 nm at a fixed total light dose 30 J/cm^2 . The reduction of living bacteria in each sample was determined by the calculation log reduction factors as follows:

$RF = \text{Log } L(-)P(-) - \text{Log } L(+)P(+)$, where $L(-)P(-)$ – no irradiation, no Pc+ (negative control); $L(+)P(+)$ – irradiation, Pc+.

2.10. Microtox® analysis

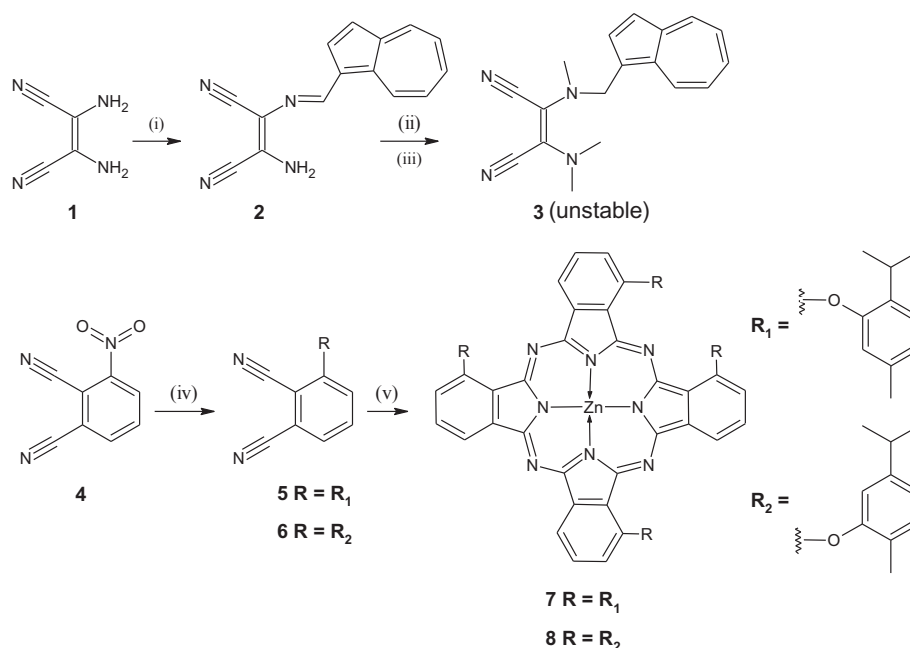
Experiments were performed according to 81.9% Microtox® test protocol with Microtox Model 500 analyzer and MicrotoxOmni software (Modern Water, Inc.) [55,56].

3. Results and discussion

3.1. Synthesis and characteristics

An attempt towards novel terpene-macrocycle conjugate was performed. In the first approach, the azulene-diaminomaleonitrile conjugate was successfully synthesized using 1-azulenecarbaldehyde and diaminomaleonitrile (Scheme 1). The resulting Schiff base compound **2** was carefully characterized and subsequently reduced and methylated to the novel derivative **3**. Unfortunately, conjugate **3** turned out to be very unstable during characterization (access to air). Moreover, even if compound **3** was quickly purified and immediately subjected to macrocyclization reaction following the conditions: magnesium *n*-butanolate in *n*-butanol, no progress of the reaction was observed. It seems that the proposed azulene-diaminomaleonitrile conjugate is not stable enough as the chemical entity thus it cannot be considered as an intermediate in the macrocyclization reaction conditions. As the continuation of the study, another approach towards terpene-macrocycle conjugate was proposed. Namely, 3-nitrobenzene-1,2-dicarbonitrile was combined with thymol or carvacrol using nitro-group displacement reaction conditions (K_2CO_3 as a base in DMF at 50 °C for 24 h) (Scheme 1) [57]. The resulting conjugates **5** and **6** were subjected to macrocyclization reactions in a microwave reactor to give phthalocyanines **7** and **8**, which were carefully purified by column chromatography and their purity was subsequently analyzed using HPLC (see Supporting Information). It is worth to note that both macrocyclization reactions were conducted without addition of DBU as a base. Experiments with DBU either failed to result in the macrocyclic product, or the reaction yields were very low. It seems that the basicity of substrates, like zinc (II) acetate was enough for the occurrence of cyclotetramerization reaction.

Thymol-phthalonitrile conjugate **5** has been previously synthesized by Ma et al. [45], and also subjected to the macrocyclization reaction. Since **5** is unsymmetrical, it can condensate in two ways. That is why Ma et al. [45] obtained an inseparable mixture of four constitutional isomers (randomers) $\text{D}_{2h} \cdot \text{C}_s \cdot \text{C}_{2v} \cdot \text{C}_{4h}$, which were formed in different



Scheme 1. Synthesis of terpene-phthalocyanine conjugates **7** and **8**. Reagents and conditions: (i) azulenicarbaldehyde, TFA, rt; (ii) NaBH₄, MeOH, rt; (iii) Me₂SO₄, DMF, –18 °C to rt; (iv) thymol or carvacrol, K₂CO₃, DMF, 50 °C, 24 h; (v) Zn(CH₃COO)₂, *n*-pentanol, MW, 200 °C, 15 min.

proportions 1:4:2:1 (Scheme 1S, Supporting Information). It is challenging to isolate specific isomer after macrocyclization reaction during typical flash column chromatography. HPLC was proved to be the best and most successful method of separation, which has been presented by Hanack and his co-workers [58]. They successfully separated for the first time the C_{4h} and the D_{2h} isomers, which was possible due to the developed HPLC phases based on π - π interactions. Surprisingly, in our work, for both substrates **5** and **6**, only one macrocyclic product was found in the reaction mixture. It is worth noting that, no other macrocyclic compounds were found during thin layer chromatography and HPLC analysis. Moreover, both isolated phthalocyanines **7** and **8** were found to be isomers of C_{2v} symmetry, which was confirmed by NMR studies. Similar situations when only one product was isolated after the macrocyclization reaction with unsymmetrical phthalonitrile have not been often reported in the literature. It has happened only for phthalonitriles with bulky substituents in the 3rd or 4th position. One of the most interesting examples was published by Lv et al. [59], who successfully isolated “pinwheel-like” menthol-substituted phthalocyanine of C_{4h} symmetry. They have performed macrocyclization reaction procedure with (D)- and (L)-3-(2-isopropyl-5-methylcyclohexoxy)-1,2-dicyanobenzene in refluxing *n*-pentanol in the presence of lithium *n*-pentanolate followed by treatment with acetic acid. Noteworthy, in our earlier work, a metronidazole-phthalocyanine conjugate of C_{2v} symmetry has been the only isomer isolated after applying the Linstead macrocyclization procedure starting from 1-[2-(2,3-dicyanophenoxy)ethyl]-2-methyl-5-nitro-1*H*-imidazole. That time only a tiny amount of another macrocyclic product was found (presumably one of the other isomers C_s, D_{2h}, C_{4h}) in the crude reaction mixture analyzed by TLC, not allowing for separation [57].

In the ¹H NMR spectrum of phthalocyanine **7**, two characteristic multiplets at 4.07 and 3.69 ppm were assigned to two pairs of CH isopropyl groups protons (marked as **A** in Fig. 1). This fact suggests that the macrocyclic molecule possesses one axis of symmetry. Considering all possible isomers (see Scheme 1S, Supporting Information), only C_{2v} isomer reveals this characteristic feature in the ¹H NMR spectrum. In the ¹H-¹H COSY spectrum both CH isopropyl peaks at 4.07 and 3.69 ppm correlate with another two aliphatic CH₃ isopropyl group protons (marked as **B**) at 1.64 and 1.14 ppm. Unlike, two signals at 2.24 and 2.27 ppm do not correlate with other signals, indicating that they

belong to methyl groups directly substituted to the aromatic ring of thymol moiety. The ¹H NMR spectrum of pc **8** represents a similar pattern. Nevertheless, protons of 2-methyl groups (**F**, Fig. 1) at ca. 2.28 and 2.87 ppm are separated. Also, one of these signals at 2.87 ppm overlaps with isopropyl proton signal marked as **D**. To sum up, in the ¹H NMR spectra of pc **7** and **8** a split of certain signals is strongly marked. Especially diagnostic are separated signals belonging to methyl groups (**C** and **F**, Fig. 1). In the case of pc **7** one slightly split signal can be observed in the ¹H NMR spectrum, whereas in the case of pc **8** two separated signals appear. We stipulate that this may be the result of steric hindrance between two terpenoid groups oriented to the same side of symmetry axis, which limits free rotation of terpenoid moieties around phenolic O–C bonds. Also, the isopropyl groups in *ortho* positions of pc **7**, as well as the methyl groups in *ortho* positions of pc **8**, can also hinder the rotation around phenolic O–C bonds in a very different manner due to the steric hindrance (phthalocyanine ring).

3.2. Spectroscopic and photochemical properties

Absorption spectra of studied compounds **7** and **8** are typical for phthalocyanines (Fig. 2). In the UV–Vis spectra of both molecules there can be recognized the Soret bands in the range of 200–400 nm and the Q bands in the range of 600–800 nm. Interestingly, phthalocyanine substituted with thymol (**7**) possesses a similar absorption profile to phthalocyanine substituted with carvacrol (**8**) presumably to the same electron donating/withdrawing properties of these groups. The terpene electron donating groups of phthalocyanines **7** and **8** ($\lambda_{Qmax} = 709$ nm) cause red-shift of the Q band in comparison to ZnPc ($\lambda_{Qmax} = 670$ nm in DMF). This effect has been recently discussed by Topal and co-workers [60]. Phthalocyanine derivatives **7** and **8** reveal emission in the red region of the UV–Vis spectrum (Fig. 1). Their excitation spectrum is comparable to the absorption one. Thus it can be concluded that in the excited state the molecules are not deformed. Moreover, this observation gives the evidence for the purity of the studied samples. The calculated fluorescence quantum yields of **7** and **8** are 2-fold lower than those measured for ZnPc (Table 1). A similar data were presented by Aliosman and co-workers for compound **I** in DMF [61]. Interestingly, compounds **7** and **8** dissolved in DMSO reveal a dramatic drop in the light emission ($\Phi_{FL} = 0.02$ for **7** and $\Phi_{FL} = 0.03$ for **8**) in comparison to

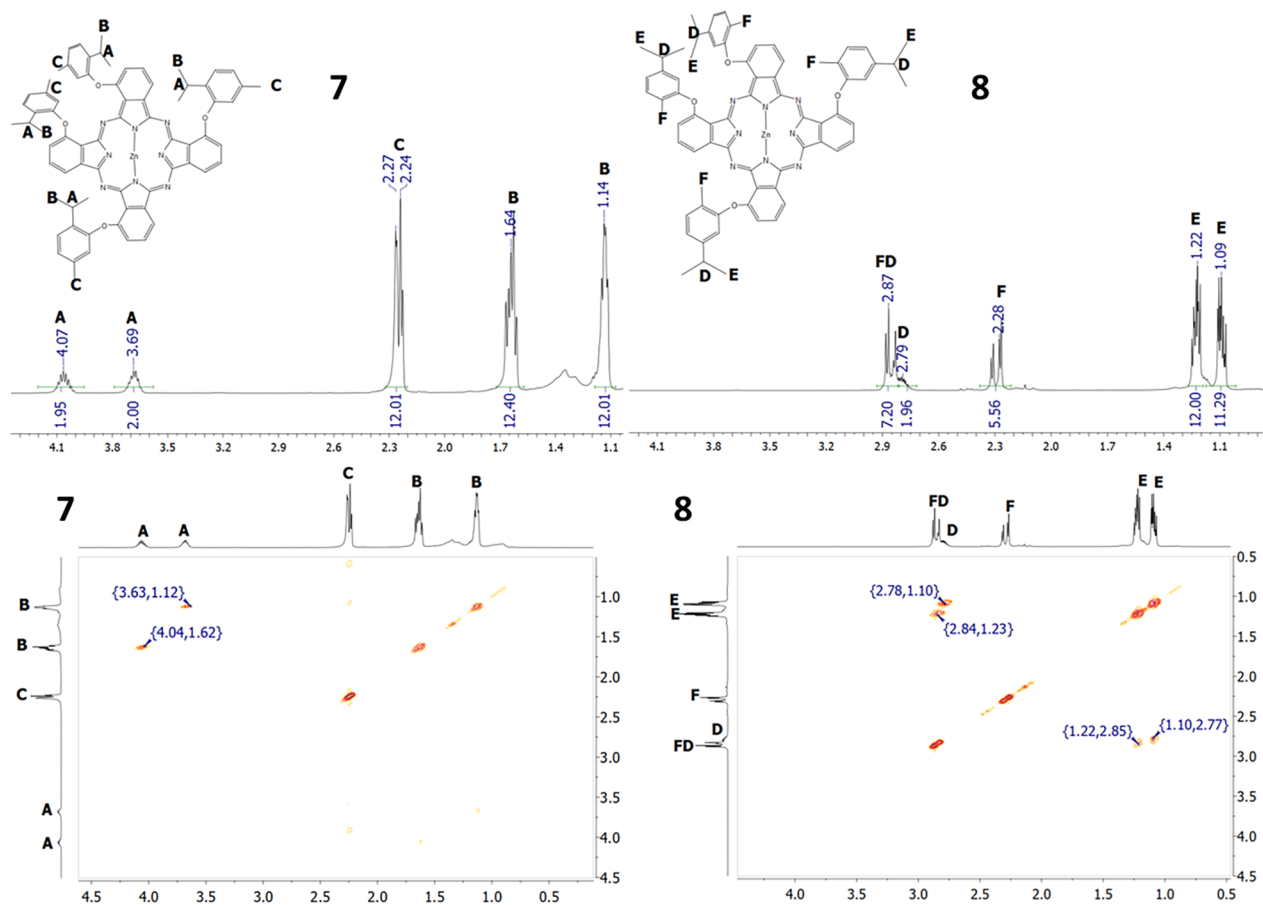


Fig. 1. ^1H NMR and ^1H - ^1H COSY spectra expansions of **7** and **8** in pyridine- d_5 in the region 1.10–4.10 ppm.

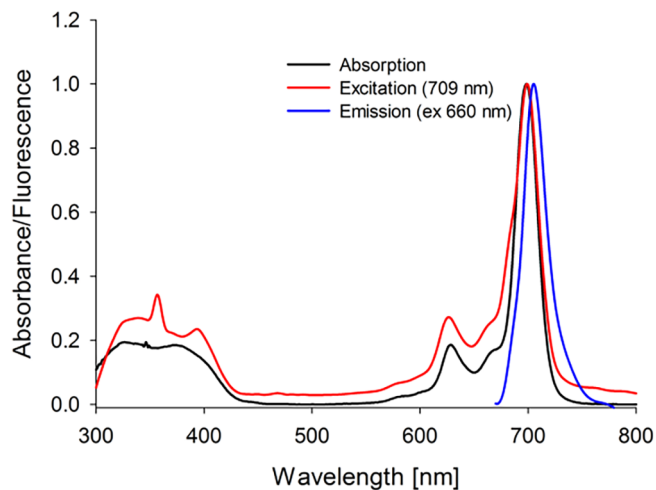


Fig. 2. Absorption, emission and excitation spectra of **7** in DMF.

ZnPc ($\Phi_{\text{FL}} = 0.17$). A similar effect has been observed by Güzel and co-workers for substituted zinc(II) phthalocyanine [5].

Both studied macrocycles generate singlet oxygen. Thus, they can be considered as potential photosensitizers for photodynamic therapy, including bacteria photoinactivation. Phthalocyanine derivative **7** forms singlet oxygen slightly better than **8**. In comparison to unsubstituted zinc(II) phthalocyanine both studied compounds (**7**, **8**) present a dramatic drop in singlet oxygen formation quantum yields – see Table 1. This phenomenon may be linked with the above discussed

Table 1

Quantum yields of fluorescence, photodecomposition and singlet oxygen formation for **7**, **8** and reference compound **ZnPc**.

Compound	Solvent	Φ_{FL}	$10^6 \Phi_{\text{p}}$	Φ_{Δ}
7	DMF	0.11	17.40	0.15
	DMSO	0.02	3.06	0.18
8	DMF	0.08	23.90	0.15
	DMSO	0.03	4.01	0.13
ZnPc	DMF	0.20 [40]	10.20	0.56 [41]
	DMSO	0.17 [40]	3.50	0.67 [41]

steric hindrance appearing between the macrocyclic ring and bulky rotating terpene substituents. This steric hindrance can also block access of molecular oxygen to the phthalocyanine core and as a consequence the singlet oxygen formation. It is known that the collision of molecular oxygen with the porphyrinoid core is essential for the formation of singlet oxygen [62]. It was proved that the periphery of the phthalocyanine can hamper access of molecular oxygen to the macrocyclic core efficiently [63]. Interestingly, Aliosman and co-workers have presented compound **I** (Fig. 3) with singlet oxygen formation quantum yield $\Phi_{\Delta} = 0.31$ in DMF [61]. The phthalocyanine derivatives **7**, **8** and phthalocyanine **I** possess phenyloxy substituents. The peripheral substituents of **I** are bulkier and exhibit much stronger electron withdrawing properties, which are essential for the enhancement of singlet oxygen formation abilities [5]. Thus, for **7** and **8** it was observed a decrease of Φ_{Δ} in comparison to unsubstituted zinc(II) phthalocyanine as a result of steric hindrance. Moreover, steric hindrance impacts the singlet oxygen formation which was indicated by Erdoğan and co-workers [64]. Also, for compound **II** a 2-fold decrease of Φ_{Δ} has been

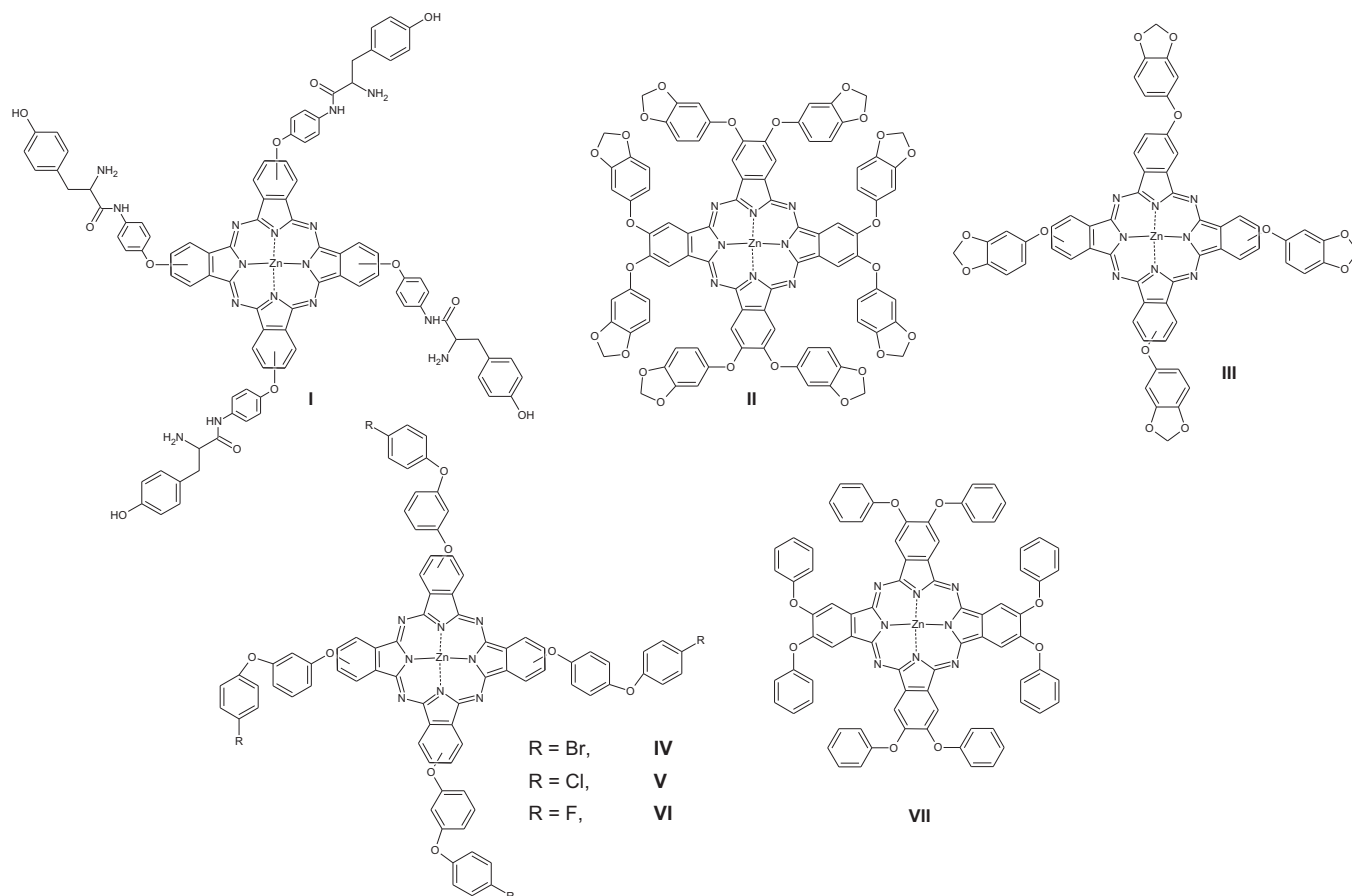


Fig. 3. Structures of phthalocyanines I-VII.

observed as compared to **III** [64]. On the other hand, a 2-fold higher Φ_{Δ} of **I** in comparison to **7** and **8** can be explained by its stronger effect of electron-donating substituents [5,60]. Kirbaç and co-workers have demonstrated the influence of electron donating/withdrawing strength of substituents for phthalocyanines **IV-VI** in DMF [65]. The substituents of compound **IV** have exhibited lowest electron withdrawing potential (highest donating) and revealed $\Phi_{\Delta} = 0.70$, whereas **V**'s $\Phi_{\Delta} = 0.72$ and finally **VI**'s $\Phi_{\Delta} = 0.95$ with highest withdrawing properties (lowest donating) within studied series. Interestingly, this tendency has not been observed in DMSO and THF solutions, which can be linked with solvent-molecule interactions [65]. Peripherally substituted phthalocyanine (**VII**) with phenoxy groups has been studied by Ogunsipe and co-workers. This molecule generated singlet oxygen with quantum yield values of 0.60 and 0.53 in DMSO and DMF respectively [48]. In comparison to **7** and **8**, compound **VII** differs slightly in the structure. Compounds **7** and **8** represent phthalocyanines substituted in the non-peripheral positions and possess alkyl groups in the bulky peripheral substituents, which potentiates steric hindrance effect, whereas phthalocyanine **VII** is substituted at peripheral positions, which generates lower steric hindrance effect. Thus, compared to **7** and **8** are weaker singlet oxygen generators than **VII**.

Irradiated phthalocyanines can undergo phototransformation or photobleaching process [66]. Compounds **7** and **8** under continuous illumination with visible light lose their colour. This observation enables to classify photodecomposition of studied phthalocyanines as photobleaching. Both phthalocyanines underwent photodecomposition with similar photodecomposition quantum yields, see Table 1. Interestingly, in comparison to the unsubstituted zinc(II) phthalocyanine, both phthalocyanine derivatives **7** and **8** revealed 2-fold lower photostability. It is worth mentioning that their singlet oxygen formation abilities were 3-fold lower than reference **ZnPc**. Mentioned dependence

was presented for samples dissolved in DMF. Compound **I** (presented in Fig. 1), in comparison to **7** and **8**, has shown much higher photodecomposition rate in DMF equal $\Phi_p = 2.54 \cdot 10^{-4}$ [61]. A similar tendency was observed for compounds **II** and **III**. In DMSO solutions compound **III** has revealed $\Phi_p = 1.02 \cdot 10^{-6}$ quantum yield and **II** $\Phi_p = 8.53 \cdot 10^{-6}$ [64]. Compounds **IV**, **V** and **VI** in comparison to **ZnPc** ($\Phi_p = 10.2 \cdot 10^{-6}$) have revealed higher photodecomposition rates with quantum yields in DMF equal $\Phi_p = 20.0 \cdot 10^{-4}$, $\Phi_p = 4.0 \cdot 10^{-4}$ and $\Phi_p = 73.0 \cdot 10^{-4}$ respectively [65]. Considering the above observations, it seems that the higher number or the bigger size of substituents can be responsible for more intensive tensions in the excited state of the molecule and stimulate the decomposition. This hypothesis needs further studies, mainly conducted with molecular calculations. Otherwise, compounds revealed similar photostability in DMSO, what can be connected to the coordination of DMSO to the central metal ion [48,52,64,65].

Terpene-phthalocyanine derivatives **7** and **8** were loaded into the modified liposomes. Also, there were prepared formulations containing unsubstituted zinc(II) phthalocyanine (**ZnPc**), thymol and carvacrol. The mean size and the size distribution of the formulation are shown in Table 2.

Thymol-phthalocyanine conjugate **7** at both 100 and 10 μM concentrations revealed high photoinactivation of *Enterococcus faecalis* of ca. 5-log growth reduction. Similar observations were made for reference compound **ZnPc**. Thus, it can be concluded that attachment of the thymol to the phthalocyanine ring does not increase its activity. Interestingly, for carvacrol-phthalocyanine conjugate **8**, an increase of its activity at 100 μM was observed in comparison to **ZnPc** and a decrease of the activity at the concentration of 10 μM – see Table 2. The drug-free liposomes, thymol and carvacrol loaded ones did not reveal significant activity. It is important that both studied phthalocyanines

Table 2
Size of the lipid vesicles and their potential for photoinactivation of *Enterococcus faecalis*.

	conditions	Photoinactivation of <i>E. faecalis</i> RF*		Size of the modified liposomes			
		100 μ M	10 μ M	Mean diameter [nm]	Dv10	Dv50	Dv90
7	light	4.72	5.02	282	136	209	529
	dark	0.08	0.01				
8	light	6.02	3.71	161	120	152	200
	dark	0.00	-0.03				
ZnPc	light	5.24	4.85	107	62	106	139
	dark	0.00	0.10				
empty liposomes	light	0.34	-0.05	122	74	123	161
	dark	0.00	0.00				
thymol	light	0.13	-0.02	166	131	159	193
	dark	0.06	-0.05				
carvacrol	light	0.39	0.39	177	132	163	249
	dark	-0.08	-0.07				

RF - * logarithmic reduction factor.

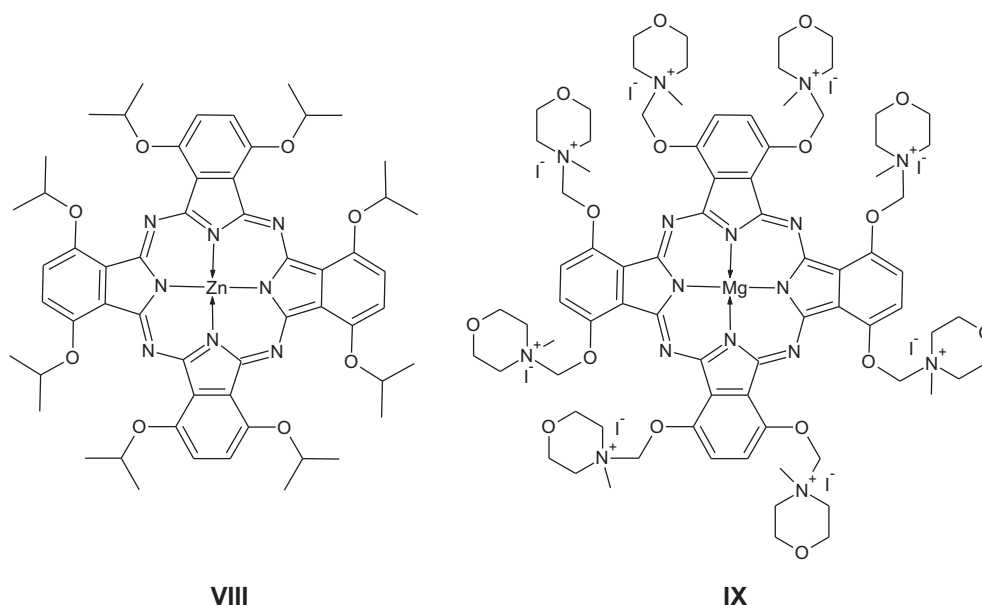


Fig. 4. Chemical structures of compounds published earlier VIII, and IX [70,71]

cross the border of 3-log photoinactivation, which is characteristic for the bactericidal agents following FDA (Food and Drug Administration) regulations [7,67,68]. Some authors have also suggested the level of 4-log for bactericidal compounds [69], which was also achieved by 7 and 8. Both phthalocyanines 7 and 8 similarly to the compounds VIII and IX (recently published by our group) revealed high photoactivity against *E. faecalis* [70,71] (Fig. 4).

The ideal photosensitizer for PACT should be inactive in the dark conditions, what is crucial for the treatment selectivity [72–74]. Therefore, Microtox® bioassay for 7 and 8 was performed. This fast and easy protocol enables to detect the acute and prolonged toxic effect of the examined agent. It is based on bioluminescent bacteria *Vibrio fischeri*, which under exposition to the toxic molecules lose its luminescent ability [55,56,75].

Terpene-phthalocyanine conjugates 7 and 8 revealed a decreased dark toxicity in comparison to the pure thymol and carvacrol (Fig. 5). Thymol and carvacrol are known to increase the permeability of the bacterial membrane leading to bacteria death [36]. As mentioned above, 7 and 8 revealed only reduced dark toxicity, which can be explained by lower bacterial membrane penetration of big phthalocyanine molecules in comparison to higher permeability of terpenes. Also, 7 revealed decreased toxicity in comparison to ZnPc and 8.

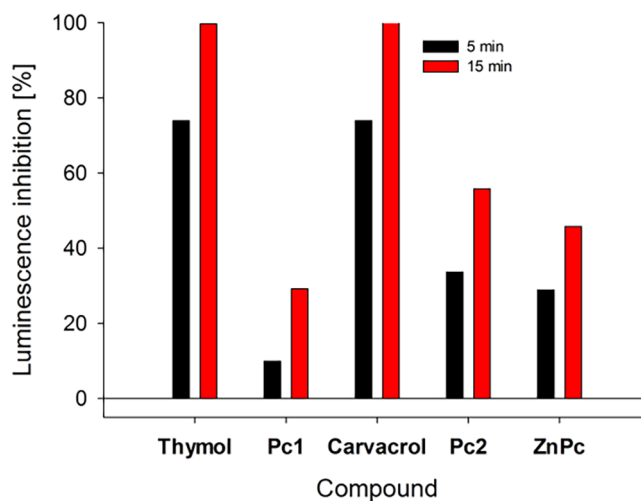


Fig. 5. *Vibrio fischeri* luminescence inhibition in Microtox® analysis.

4. Conclusion

In our initial study an attempt towards novel terpene-macrocyclic conjugate, consisting of phthalocyanine and azulene was performed. This attempt was abandoned on the stage of azulene-maleonitrile derivative substrate macrocyclization reaction, which turned out to be very unstable during characterization and macrocyclization reaction reconnaissance study. Another approach towards terpene-macrocyclic conjugate was successfully performed when 3-nitrobenzene-1,2-dicarbonitrile was conjugated with thymol or carvacrol using nitro-group displacement procedure and when the resulting conjugates were subsequently subjected to macrocyclization reactions in a microwave reactor towards desired terpene-phthalocyanine conjugates. It is worth to note that both reactions were conducted without addition of DBU as a base. Experiments with DBU either failed to result with the macrocyclic product or the reaction yields were very low. It seems that the basicity of substrates, like zinc(II) acetate was enough for the occurrence of cyclotetramerization reaction. The obtained compounds were characterized by UV–Vis, NMR, MS, and HPLC. It is interesting that in the referenced approach by Ma et al. [45], a thymol-phthalonitrile conjugate when subjected to the macrocyclization reaction led to the mixture of thymol-phthalocyanine randomers. Surprisingly, in our work, for both phthalonitrile derivatives, only one macrocyclic product of C_{2v} symmetry was found in the reaction mixture. The structure of the macrocyclic product was unambiguously confirmed in the NMR study. For both compounds, diagnostic signals belonging to isopropyl and methyl groups of terpene substituents were identified.

Absorption spectra of studied compounds are typical for phthalocyanines with the Soret the Q band and possess the same profile. This phenomenon is linked to the same electron donating/withdrawing properties of substituents. Studied phthalocyanines reveal emission in the red region of UV–Vis spectrum with calculated fluorescence quantum yields about 2-fold lower than that for ZnPc. Interestingly, compounds dissolved in DMSO presented a dramatic drop in light emission. Among studied compounds thymol-phthalocyanine conjugate generated singlet oxygen slightly more efficiently than carvacrol-phthalocyanine conjugate. Nevertheless, in comparison with unsubstituted zinc(II) phthalocyanine both studied compounds presented a decrease in singlet oxygen formation quantum yields. This phenomenon may be linked with steric hindrance formed by rotating substituents. Both terpene-phthalocyanine conjugates under illumination with visible light continuously lose their colour, which enables to classify photodecomposition of studied molecules as photobleaching. Both phthalocyanines underwent photodecomposition with similar photodecomposition quantum yield. Interestingly, in comparison to the unsubstituted zinc(II) phthalocyanine, both terpene-phthalocyanine conjugates revealed 2-fold lower photostability and 3-fold lower singlet oxygen formation ability in DMF. It seems that higher number or bigger size of substituents is responsible for more intensive tensions in the excited state of the molecule and stimulates the decomposition. Otherwise, in DMSO compounds revealed similar photostability, which can be the result of coordination of DMSO to the central metal ion. Both phthalocyanine analogs were loaded to the modified liposomes. Formulations containing unsubstituted zinc(II) phthalocyanine, thymol and carvacrol were obtained as well. Thymol-phthalocyanine conjugate at both 100 and 10 μ M revealed high photoinactivation growth of *Enterococcus faecalis* at ca. 5-log, similarly to reference ZnPc. For carvacrol-phthalocyanine conjugate, an increase of activity at 100 μ M in comparison to ZnPc was observed and a decrease at 10 μ M. Both studied conjugates cross the border of 3-log, which indicates their bactericidal potential according to the FDA regulations. The Microtox[®] bioassay was performed for both conjugates revealing their low dark toxicity, which was significantly below the dark toxicity measured for the pure thymol and carvacrol.

Acknowledgments

This work has been supported by the National Science Centre, Poland through grant No. 2015/19/N/NZ7/01342.

Appendix A. Supplementary data

Supplementary data to this article can be found online at <https://doi.org/10.1016/j.ica.2019.02.031>.

References

- [1] D. Wöhrle, G. Schnurpfeil, S.G. Makarov, A. Kazarin, O.N. Suvorova, Practical applications of phthalocyanines – from dyes and pigments to materials for optical electronic and photo-electronic devices, *Macromolecules* 5 (2012) 191–202, <https://doi.org/10.6060/mhc2012.120990w>.
- [2] A. Günsel, E. Güzel, A.T. Bilgiçli, İ. Şişman, M.N. Yarasir, Synthesis of non-peripheral thioanisole-substituted phthalocyanines: photophysical, electrochemical, photovoltaic, and sensing properties, *J. Photochem. Photobiol. Chem.* 348 (2017) 57–67, <https://doi.org/10.1016/j.jphotochem.2017.07.040>.
- [3] S. Yano, S. Hirohara, M. Obata, Y. Hagiya, S. Ogura, A. Ikeda, H. Kataoka, M. Tanaka, T. Joh, Current states and future views in photodynamic therapy, *J. Photochem. Photobiol. C Photochem. Rev.* 12 (2011) 46–67, <https://doi.org/10.1016/j.jphotochemrev.2011.06.001>.
- [4] C.M. Cassidy, M.M. Tunney, P.A. McCarron, R.F. Donnelly, Drug delivery strategies for photodynamic antimicrobial chemotherapy: from benchtop to clinical practice, *J. Photochem. Photobiol. B* 95 (2009) 71–80, <https://doi.org/10.1016/j.jphotobiol.2009.01.005>.
- [5] E. Güzel, A. Günsel, A.T. Bilgiçli, G.Y. Atmaca, A. Erdoğan, M.N. Yarasir, Synthesis and photophysical properties of novel thiadiazole-substituted zinc (II), gallium (III) and silicon (IV) phthalocyanines for photodynamic therapy, *Inorg. Chim. Acta* 467 (2017) 169–176, <https://doi.org/10.1016/j.ica.2017.07.058>.
- [6] T. Maisch, A new strategy to destroy antibiotic resistant microorganisms: antimicrobial photodynamic treatment, *Mini Rev. Med. Chem.* 9 (2009) 974–983, <https://doi.org/10.2174/138955709788681582>.
- [7] L. Sobotta, P. Skupin-Mrugalska, J. Piskorz, J. Mielcarek, Non-porphyrinoid photosensitizers mediated photodynamic inactivation against bacteria, *Dyes Pigm.* 163 (2019) 337–355, <https://doi.org/10.1016/j.dyepig.2018.12.014>.
- [8] A. Tillo, M. Stolarska, M. Kryjewski, L. Popenka, L. Sobotta, S. Jurga, J. Mielcarek, T. Goslinski, Phthalocyanines with bulky substituents at non-peripheral positions – synthesis and physico-chemical properties, *Dyes Pigm.* 127 (2016) 110–115, <https://doi.org/10.1016/j.dyepig.2015.12.017>.
- [9] L. Ryskova, V. Buchta, M. Karaskova, J. Rakusan, J. Cerny, R. Slezak, In vitro antimicrobial activity of light-activated phthalocyanines, *Cent. Eur. J. Biol.* 8 (2013) 168–177, <https://doi.org/10.2478/s11535-013-0118-0>.
- [10] A. Sindelo, O.L. Osifeko, T. Nyokong, Synthesis, photophysical and photodynamic antimicrobial chemotherapy studies of indium pyridyl phthalocyanines: charge versus bridging atom, *Inorg. Chim. Acta* 476 (2018) 68–76, <https://doi.org/10.1016/j.ica.2018.02.020>.
- [11] M. Li, B. Mai, A. Wang, Y. Gao, X. Wang, X. Liu, S. Song, Q. Liu, S. Wei, P. Wang, Photodynamic antimicrobial chemotherapy with cationic phthalocyanines against *Escherichia coli* planktonic and biofilm cultures, *RSC Adv.* 7 (2017) 40734–40744, <https://doi.org/10.1039/C7RA06073D>.
- [12] Y. Gao, B. Mai, A. Wang, M. Li, X. Wang, K. Zhang, Q. Liu, S. Wei, P. Wang, Antimicrobial properties of a new type of photosensitizer derived from phthalocyanine against planktonic and biofilm forms of *Staphylococcus aureus*, *Photodiagn. Photodyn. Ther.* 21 (2018) 316–326, <https://doi.org/10.1016/j.pdpdt.2018.01.003>.
- [13] C. Uslan, N.D. İşleyen, Y. Öztürk, B.T. Yıldız, Z.P. Çakar, M. Göksel, M. Durmuş, Y.H. Gürsel, B.Ş. Sesalan, A novel of PEG-conjugated phthalocyanine and evaluation of its photocytotoxicity and antibacterial properties for photodynamic therapy, *J. Porphyr. Phthalocyanines* 22 (2018) 10–24, <https://doi.org/10.1142/S1088424617500729>.
- [14] B.-Y. Zheng, X.-J. Jiang, T. Lin, M.-R. Ke, J.-D. Huang, Novel silicon(IV) phthalocyanines containing piperidinyl moieties: synthesis and in vitro antifungal photodynamic activities, *Dyes Pigments* 112 (2015) 311–316, <https://doi.org/10.1016/j.dyepig.2014.07.029>.
- [15] B.-Y. Zheng, T. Lin, H.-H. Yang, J.-D. Huang, Photodynamic inactivation of *Candida albicans* sensitized by a series of novel axially di-substituted silicon (IV) phthalocyanines, *Dyes Pigm.* 96 (2013) 547–553, <https://doi.org/10.1016/j.dyepig.2012.09.013>.
- [16] M.-R. Ke, J.M. Eastel, K.L.K. Ngai, Y.-Y. Cheung, P.K.S. Chan, M. Hui, D.K.P. Ng, P.-C. Lo, Oligolysine-conjugated zinc(II) phthalocyanines as efficient photosensitizers for antimicrobial photodynamic therapy, *Chem. - Asian J.* 9 (2014) 1868–1875, <https://doi.org/10.1002/asia.201402025>.
- [17] Z. Chen, S. Zhou, J. Chen, L. Li, P. Hu, S. Chen, M. Huang, An effective zinc phthalocyanine derivative for photodynamic antimicrobial chemotherapy, *J. Lumin.* 152 (2014) 103–107, <https://doi.org/10.1016/j.jlumin.2013.10.067>.
- [18] G.B. Rodrigues, F.L. Primo, A.C. Tedesco, G.U.L. Braga, In vitro photodynamic

- inactivation of cryptococcus neoformans melanized cells with chloroaluminum phthalocyanine nanoemulsion, *Photochem. Photobiol.* 88 (2012) 440–447, <https://doi.org/10.1111/j.1751-1097.2011.01055.x>.
- [19] L. Sobotta, J. Długaszewska, P. Kasprzycki, S. Lijewski, A. Teubert, J. Mielcarek, M. Gdaniec, T. Goslinski, P. Fita, E. Tykarska, *In vitro* photodynamic activity of lipid vesicles with zinc phthalocyanine derivative against *Enterococcus faecalis*, *J. Photochem. Photobiol. B* 183 (2018) 111–118, <https://doi.org/10.1016/j.jphotochem.2018.04.025>.
- [20] L. Sobotta, J. Sniechowska, D. Ziental, J. Długaszewska, M.J. Potrzebowski, Chlorins with (trifluoromethyl)phenyl substituents – synthesis, lipid formulation and photodynamic activity against bacteria, *Dyes Pigm.* 160 (2019) 292–300, <https://doi.org/10.1016/j.dyepig.2018.08.004>.
- [21] L. Sobotta, J. Długaszewska, M. Gierszewski, A. Tillo, M. Sikorski, E. Tykarska, J. Mielcarek, T. Goslinski, Photodynamic inactivation of *Enterococcus faecalis* by non-peripherally substituted magnesium phthalocyanines entrapped in lipid vesicles, *J. Photochem. Photobiol. B* 188 (2018) 100–106, <https://doi.org/10.1016/j.jphotochem.2018.09.003>.
- [22] L. Sobotta, J. Długaszewska, D. Ziental, W. Szczolko, T. Koczorowski, T. Goslinski, J. Mielcarek, Optical properties of a series of pyrrolyl-substituted porphyrins and their photoinactivation potential against *Enterococcus faecalis* after incorporation into liposomes, *J. Photochem. Photobiol. Chem.* 368 (2019) 104–109, <https://doi.org/10.1016/j.jphotochem.2018.09.015>.
- [23] L. Sobotta, D. Ziental, J. Sniechowska, J. Długaszewska, M.J. Potrzebowski, Lipid vesicle-loaded *meso*-substituted chlorins of high *in vitro* antimicrobial photodynamic activity, *Photochem. Photobiol. Sci.* (2019), <https://doi.org/10.1039/C8PP00258D>.
- [24] S. Koch, M. Hufnagel, C. Theilacker, J. Huebner, Enterococcal infections: host response, therapeutic, and prophylactic possibilities, *Vaccine* 22 (2004) 822–830, <https://doi.org/10.1016/j.vaccine.2003.11.027>.
- [25] C.M.A.P. Franz, A.B. Muscholl-Silberhorn, N.M.K. Yousif, M. Vancanneyt, J. Swings, W.H. Holzappel, Incidence of virulence factors and antibiotic resistance among enterococci isolated from food, *Appl. Environ. Microbiol.* 67 (2001) 4385–4389, <https://doi.org/10.1128/AEM.67.9.4385-4389.2001>.
- [26] I. Kühn, Comparison of enterococcal populations in animals, humans, and the environment – a European study, *Int. J. Food Microbiol.* 88 (2003) 133–145, [https://doi.org/10.1016/S0168-1605\(03\)00176-4](https://doi.org/10.1016/S0168-1605(03)00176-4).
- [27] R. Souto, A.P.V. Colombo, Prevalence of *Enterococcus faecalis* in subgingival biofilm and saliva of subjects with chronic periodontal infection, *Arch. Oral Biol.* 53 (2008) 155–160, <https://doi.org/10.1016/j.archoralbio.2007.08.004>.
- [28] R.M. Love, *Enterococcus faecalis* – a mechanism for its role in endodontic failure, *Int. Endod. J.* 34 (2001) 399–405, <https://doi.org/10.1046/j.1365-2591.2001.00437.x>.
- [29] C.A. Arias, B.E. Murray, The rise of the *Enterococcus*: beyond vancomycin resistance, *Nat. Rev. Microbiol.* 10 (2012) 266–278, <https://doi.org/10.1038/nrmicro2761>.
- [30] H.-M. Chiang, J.-J. Yin, Q. Xia, Y. Zhao, P.P. Fu, K.-C. Wen, H. Yu, Photoirradiation of azulene and guaiazulene—formation of reactive oxygen species and induction of lipid peroxidation, *J. Photochem. Photobiol. Chem.* 211 (2010) 123–128, <https://doi.org/10.1016/j.jphotochem.2010.02.007>.
- [31] R.R.A. Hayek, N.S. Araújo, M.A. Gioso, J. Ferreira, C.A. Baptista-Sobrinho, A.M. Yamada, M.S. Ribeiro, Comparative study between the effects of photodynamic therapy and conventional therapy on microbial reduction in ligature-induced peri-implantitis in dogs, *J. Periodontol.* 76 (2005) 1275–1281, <https://doi.org/10.1902/jop.2005.76.8.1275>.
- [32] B. Salehi, A.P. Mishra, I. Shukla, M. Sharifi-Rad, M. del M. Contreras, A. Segura-Carretero, H. Fathi, N.N. Nasrabadi, F. Kobarfard, J. Sharifi-Rad, Thymol, thyme, and other plant sources: health and potential uses: thymol, health and potential uses, *Phytother. Res.* 32 (2018) 1688–1706, <https://doi.org/10.1002/ptr.6109>.
- [33] M. Sharifi-Rad, E.M. Varoni, M. Iriti, M. Martorell, W.N. Setzer, M. del Mar Contreras, B. Salehi, A. Soltani-Nejad, S. Rajabi, M. Tajbakhsh, J. Sharifi-Rad, Carvacrol and human health: a comprehensive review: carvacrol and Human Health, *Phytother. Res.* 32 (2018) 1675–1687, <https://doi.org/10.1002/ptr.6103>.
- [34] M.Y. Memar, P. Raei, N. Alizadeh, M. Akbari Aghdam, H.S. Kafil, Carvacrol and thymol: strong antimicrobial agents against resistant isolates, *Rev. Med. Microbiol.* 28 (2017) 63–68, <https://doi.org/10.1097/MRM.0000000000000100>.
- [35] A. Marchese, I.E. Orhan, M. Daglia, R. Barbieri, A. Di Lorenzo, S.F. Nabavi, O. Gortzi, M. Izadi, S.M. Nabavi, Antibacterial and antifungal activities of thymol: a brief review of the literature, *Food Chem.* 210 (2016) 402–414, <https://doi.org/10.1016/j.foodchem.2016.04.111>.
- [36] A. Guarda, J.F. Rubilar, J. Miltz, M.J. Galotto, The antimicrobial activity of microencapsulated thymol and carvacrol, *Int. J. Food Microbiol.* 146 (2011) 144–150, <https://doi.org/10.1016/j.jfoodmicro.2011.02.011>.
- [37] B. Shah, S. Ikeda, P. Michael Davidson, Q. Zhong, Nanodispersing thymol in whey protein isolate-maltodextrin conjugate capsules produced using the emulsion- evaporation technique, *J. Food Eng.* 113 (2012) 79–86, <https://doi.org/10.1016/j.jfoodeng.2012.05.019>.
- [38] B. Shah, P.M. Davidson, Q. Zhong, Antimicrobial activity of nanodispersed thymol in tryptic soy broth, *J. Food Prot.* 76 (2013) 440–447, <https://doi.org/10.4315/0362-028X.JFP-12-354>.
- [39] B. Shah, P.M. Davidson, Q. Zhong, Nanodispersed eugenol has improved antimicrobial activity against *Escherichia coli* O157:H7 and *Listeria monocytogenes* in bovine milk, *Int. J. Food Microbiol.* 161 (2013) 53–59, <https://doi.org/10.1016/j.ijfoodmicro.2012.11.020>.
- [40] V.K. Redasani, S.B. Bari, Synthesis and evaluation of mutual prodrugs of ibuprofen with menthol, thymol and eugenol, *Eur. J. Med. Chem.* 56 (2012) 134–138, <https://doi.org/10.1016/j.ejmech.2012.08.030>.
- [41] S.S. Swain, S.K. Paidasetty, R.N. Padhy, Development of antibacterial conjugates using sulfamethoxazole with monocyclic terpenes: a systematic medicinal chemistry based computational approach, *Comput. Methods Programs Biomed.* 140 (2017) 185–194, <https://doi.org/10.1016/j.cmpb.2016.12.013>.
- [42] S.S. Swain, S.K. Paidasetty, R.N. Padhy, Antibacterial activity, computational analysis and host toxicity study of thymol-sulfonamide conjugates, *Biomed. Pharmacother.* 88 (2017) 181–193, <https://doi.org/10.1016/j.biopha.2017.01.036>.
- [43] R. Cahan, N. Swissa, G. Gellerman, Y. Nitzan, Photosensitizer-antibiotic conjugates: a novel class of antibacterial molecules, *Photochem. Photobiol.* 86 (2010) 418–425, <https://doi.org/10.1111/j.1751-1097.2009.00674.x>.
- [44] Z. Zhang, G.M. Ferrence, T.D. Lash, *adj*-Diazuloporphyryns, a New Family of Dicarboxyphthalocyanines with Unprecedented Mesoinic Characteristics ¹, *Org. Lett.* 11 (2009) 101–104, <https://doi.org/10.1021/ol802406f>.
- [45] C. Ma, D. Tian, X. Hou, Y. Chang, F. Cong, H. Yu, X. Du, G. Du, Synthesis and characterization of several soluble tetraphenoxy-substituted copper and zinc phthalocyanines, *ChemInform* 36 (2005), <https://doi.org/10.1002/chin.200533201>.
- [46] L. Sobotta, P. Fita, W. Szczolko, M. Wrotynski, M. Wierchowski, T. Goslinski, J. Mielcarek, Functional singlet oxygen generators based on porphyrins with peripheral 2,5-dimethylpyrrol-1-yl and dimethylamino groups, *J. Photochem. Photobiol. Chem.* 269 (2013) 9–16, <https://doi.org/10.1016/j.jphotochem.2013.06.018>.
- [47] V. Chauke, A. Ogunsipe, M. Durmuş, T. Nyokong, Novel gallium(III) phthalocyanine derivatives – synthesis, photophysics and photochemistry, *Polyhedron* 26 (2007) 2663–2671, <https://doi.org/10.1016/j.poly.2007.01.016>.
- [48] A. Ogunsipe, D. Maree, T. Nyokong, Solvent effects on the photochemical and fluorescence properties of zinc phthalocyanine derivatives, *J. Mol. Struct.* 650 (2003) 131–140, [https://doi.org/10.1016/S0022-2860\(03\)00155-8](https://doi.org/10.1016/S0022-2860(03)00155-8).
- [49] A. Ogunsipe, M. Durmuş, D. Atilla, A.G. Gürek, V. Ahsen, T. Nyokong, Synthesis, photophysical and photochemical studies on long chain zinc phthalocyanine derivatives, *Synth. Met.* 158 (2008) 839–847, <https://doi.org/10.1016/j.synthmet.2008.06.007>.
- [50] I. Seotsanyana-Mokhosi, N. Kuznetsova, T. Nyokong, Photochemical studies of tetra-2, 3-pyridinoporphyrazines, *J. Photochem. Photobiol. Chem.* 140 (2001) 215–222.
- [51] X. Shen, W. Lu, G. Feng, Y. Yao, W. Chen, Preparation and photoactivity of a novel water-soluble, polymerizable zinc phthalocyanine, *J. Mol. Catal. Chem.* 298 (2009) 17–22, <https://doi.org/10.1016/j.molcata.2008.09.023>.
- [52] N.A. Kuznetsova, V.V. Okunchikov, V.M. Derkacheva, O.L. Kaliya, E.A. Lukyanets, Photooxidation of metallophthalocyanines: the effects of singlet oxygen and Pc-M-O 2 complex formation, *J. Porphyr. Phthalocyanines* 9 (2005) 393–397.
- [53] N.A. Kuznetsova, D.A. Makarov, O.A. Yuzhakova, L.I. Solovieva, O.L. Kaliya, Study on the photostability of water-soluble Zn(II) and Al(III) phthalocyanines in aqueous solution, *J. Porphyr. Phthalocyanines* 14 (2010) 968–974, <https://doi.org/10.1142/S1088424610002835>.
- [54] N. Dragicevic-Curic, D. Scheglmann, V. Albrecht, A. Fahr, Development of different temoporfin-loaded invasomes—novel nanocarriers of temoporfin: characterization, stability and *in vitro* skin penetration studies, *Colloids Surf. B Biointerfaces* 70 (2009) 198–206, <https://doi.org/10.1016/j.colsurfb.2008.12.030>.
- [55] T.X.H. Le, T.V. Nguyen, Z. Amadou Yacouba, L. Zoungrana, F. Avril, D.L. Nguyen, E. Petit, J. Mendret, V. Bonniol, M. Bechelany, S. Lacour, G. Lesage, M. Cretin, Correlation between degradation pathway and toxicity of acetaminophen and its by-products by using the electro-Fenton process in aqueous media, *Chemosphere* 172 (2017) 1–9, <https://doi.org/10.1016/j.chemosphere.2016.12.060>.
- [56] R. Weltens, K. Deprez, L. Michiels, Validation of Microtox as a first screening tool for waste classification, *Waste Manage.* 34 (2014) 2427–2433, <https://doi.org/10.1016/j.wasman.2014.08.001>.
- [57] M. Wierchowski, L. Sobotta, P. Skupin-Mrugalska, J. Kruk, W. Jusiak, M. Yee, K. Konopka, N. Düzgüneş, E. Tykarska, M. Gdaniec, J. Mielcarek, T. Goslinski, Phthalocyanines functionalized with 2-methyl-5-nitro-1H-imidazolylethoxy and 1,4,7-trioxanonyl moieties and the effect of metronidazole substitution on photocytotoxicity, *J. Inorg. Biochem.* 127 (2013) 62–72, <https://doi.org/10.1016/j.jinorgbio.2013.06.012>.
- [58] M. Sommerauer, C. Rager, M. Hanack, Separation of 2(3),9(10),16(17),23(24)-tetrasubstituted phthalocyanines with newly developed HPLC phases, *J. Am. Chem. Soc.* 118 (1996) 10085–10093, <https://doi.org/10.1021/ja961009x>.
- [59] W. Lv, J. Duan, S. Ai, “Pinwheel-like” phthalocyanines with four non-peripheral chiral menthol units: Synthesis, spectroscopy, and electrochemistry, *Chin. Chem. Lett.* 30 (2019) 389–391, <https://doi.org/10.1016/j.ccl.2018.06.002>.
- [60] S.Z. Topal, Ü. İsci, U. Kumru, D. Atilla, A.G. Gürek, C. Hırel, M. Durmuş, J.-B. Tommasino, D. Luneau, S. Berber, F. Dumoulin, V. Ahsen, Modulation of the electronic and spectroscopic properties of Zn(II) phthalocyanines by their substitution pattern, *Dalton Trans.* 43 (2014) 6897, <https://doi.org/10.1039/c3dt53410c>.
- [61] M. Aliosman, M. Göksel, V. Mantareva, I. Stoineva, M. Durmuş, Tyrosine conjugated zinc(II) phthalocyanine for photodynamic therapy: synthesis and photochemical properties, *J. Photochem. Photobiol. Chem.* 334 (2017) 101–106, <https://doi.org/10.1016/j.jphotochem.2016.10.037>.
- [62] M.C. DeRosa, R.J. Crutchley, Photosensitized singlet oxygen and its applications, *Coord. Chem. Rev.* 233 (2002) 351–371.
- [63] G. Cheng, X. Peng, G. Hao, V.O. Kennedy, I.N. Ivanov, K. Knappenberger, T.J. Hill, M.A.J. Rodgers, M.E. Kenney, Synthesis, photochemistry, and electrochemistry of a series of phthalocyanines with graded steric hindrance, *J. Phys. Chem. A* 107 (2003) 3503–3514, <https://doi.org/10.1021/jp027006q>.
- [64] A. Erdoğan, T. Nyokong, New soluble methylenedioxy-substituted zinc

- phthalocyanine derivatives: synthesis, photophysical and photochemical studies, *Polyhedron* 28 (2009) 2855–2862, <https://doi.org/10.1016/j.poly.2009.06.019>.
- [65] E. Kırbaç, G.Y. Atmaca, A. Erdoğan, Novel highly soluble fluoro, chloro, bromo-phenoxy-phenoxy substituted zinc phthalocyanines; synthesis, characterization and photophysical properties, *J. Organomet. Chem.* 752 (2014) 115–122, <https://doi.org/10.1016/j.jorganchem.2013.12.005>.
- [66] R. Bonnett, G. Martinez, Photobleaching of sensitizers used in photodynamic therapy, *Tetrahedron* 57 (2001) 9513–9547.
- [67] E. Alves, M.A. Faustino, M.G. Neves, A. Cunha, J. Tome, A. Almeida, An insight on bacterial cellular targets of photodynamic inactivation, *Future Med. Chem.* 6 (2014) 141–164, <https://doi.org/10.4155/fmc.13.211>.
- [68] A. Spaeth, A. Graeler, T. Maisch, K. Plaetzer, CureCuma—cationic curcuminoids with improved properties and enhanced antimicrobial photodynamic activity, *Eur. J. Med. Chem.* (2017), <https://doi.org/10.1016/j.ejmech.2017.09.072>.
- [69] G. Jori, C. Fabris, M. Soncin, S. Ferro, O. Coppellotti, D. Dei, L. Fantetti, G. Chiti, G. Roncucci, Photodynamic therapy in the treatment of microbial infections: basic principles and perspective applications, *Lasers Surg. Med.* 38 (2006) 468–481, <https://doi.org/10.1002/lsm.20361>.
- [70] L. Sobotta, J. Długaszewska, P. Kasprzycki, S. Lijewski, A. Teubert, J. Mielcarek, M. Gdaniec, T. Goslinski, P. Fita, E. Tykarska, In vitro photodynamic activity of lipid vesicles with zinc phthalocyanine derivative against *Enterococcus faecalis*, *J. Photochem. Photobiol. B* (2018), <https://doi.org/10.1016/j.jphotobiol.2018.04.025>.
- [71] J. Długaszewska, W. Szczołko, T. Koczorowski, P. Skupin-Mrugalska, A. Teubert, K. Konopka, M. Kucinska, M. Murias, N. Düzgüneş, J. Mielcarek, T. Goslinski, Antimicrobial and anticancer photodynamic activity of a phthalocyanine photosensitizer with N-methyl morpholiniumethoxy substituents in non-peripheral positions, *J. Inorg. Biochem.* 172 (2017) 67–79, <https://doi.org/10.1016/j.jinorgbio.2017.04.009>.
- [72] R.R. Allison, G.H. Downie, R. Cuenca, X.-H. Hu, C.J. Childs, C.H. Sibata, Photosensitizers in clinical PDT, *Photodiagnosis Photodyn. Ther.* 1 (2004) 27–42, [https://doi.org/10.1016/S1572-1000\(04\)00007-9](https://doi.org/10.1016/S1572-1000(04)00007-9).
- [73] P. Agostinis, K. Berg, K.A. Cengel, T.H. Foster, A.W. Girotti, S.O. Gollnick, S.M. Hahn, M.R. Hamblin, A. Juzeniene, D. Kessel, M. Korbelik, J. Moan, P. Mroz, D. Nowis, J. Piette, B.C. Wilson, J. Golab, Photodynamic therapy of cancer: an update, *CA Cancer J. Clin.* 61 (2011) 250–281, <https://doi.org/10.3322/caac.20114>.
- [74] J.F. Lovell, T.W.B. Liu, J. Chen, G. Zheng, Activatable photosensitizers for imaging and therapy, *Chem. Rev.* 110 (2010) 2839–2857, <https://doi.org/10.1021/cr900236h>.
- [75] V.R. Urbano, M.G. Maniero, M. Pérez-Moya, J.R. Guimarães, Influence of pH and ozone dose on sulfaquinoxaline ozonation, *J. Environ. Manage.* 195 (2017) 224–231, <https://doi.org/10.1016/j.jenvman.2016.08.019>.